

MONITORING CARBON CONTENT COMPOSITION OF NANOPARTICLES GENERATED IN A PREMIXED ETHYLENE AIR FLAME

F. Picca*, M. Commodo, P. Minutolo**, A. D'Anna***

francesca.picca@unina.it

* Dipartimento di Ingegneria Chimica, dei Materiali e della Produzione Industriale -
Università degli Studi di Napoli Federico II, P.le Tecchio 80, 80125, Napoli, Italy

**Istituto di Scienze e Tecnologie per L'Energia e La Mobilità Sostenibili (STEMS)-CNR,
80125, Napoli, Italy

Abstract

The study investigates the composition and properties of carbonaceous nanoparticles formed in a premixed laminar ethylene-air flame. The work aims to understand the evolution of these particles within the flame, from nucleation to growth, regarding their structural composition particularly focusing on the fractions of organic carbon (OC) and elemental carbon (EC). Experimental analysis involves thermo-optical-transmission (TOT) measurements and Raman spectroscopy of particles collected at different residence times. Results reveal a prevalence of organic carbon at lower residence times, transitioning to elemental carbon at longer residence times. Raman spectroscopy confirms the presence of characteristic carbon bands and highlights variations in the fluorescence background, correlating with the dominance of organic carbon during nucleation and early particle growth. The study contributes to a deeper understanding of carbonaceous nanoparticle formation in flames and provides valuable insights into their composition and properties.

Introduction

The investigation into the formation of soot particles, categorized as carbonaceous nanoparticles, during high-temperature incomplete combustion of hydrocarbon fuels remains a central focus within the combustion research community. Studies on the properties of soot particles underscore their sensitivity to various combustion parameters [1–4]. Indeed, the flame conditions significantly influence the size and composition of the particles, which undergo complex chemical and physical transformations during fuel-rich combustion. The evolution of soot particles within flames starts from nucleation to growth and maturation, resulting in a diverse array of structural and optical characteristics. Understanding the underlying chemistry and physics of this process is paramount for mitigating carbon particle emissions from combustion systems, given the significant concerns regarding their impact on human health, environmental quality, and climate change [5]. Concurrently, the production of carbonaceous particles has spurred interest in flame synthesis, an innovative

approach for generating nanomaterials, particularly of the carbon variety [6–8]. The diverse array of generated combustion materials holds immense potential for promising advancements that can improve our quality of life. To utilize this potential there is a pressing need for a deeper understanding of the mechanisms underlying their formation. Combustion processes yield a diverse array of carbonaceous compounds starting from gas-phase polycyclic aromatic hydrocarbons (PAHs), often serving as precursors to soot particles. These PAHs, once nucleated, undergo processes of coagulation, coalescence, and mass growth through heterogeneous solid-gas phase reactions. A formation of larger particles, whose size typically increases with residence time [2], happens. The composition and properties of these particles produced at different residence times may vary, particularly in terms of organic carbon (OC) and elemental carbon (EC) fractions [9–10]. These variations in composition give rise to a range of properties that are significant for diagnostic purposes. To address these challenges, evaluating the composition of soot particles in terms of EC and OC fractions is essential. Thermo-optical-transmission (TOT) analysis serves as a standard method for quantifying carbon concentration and distinguishing between OC and EC components. Additionally, there is a need for chemical characterization of the materials under study. Raman spectroscopy offers valuable insights into the chemical structural evolution of various nanoparticles in terms of their molecular composition and arrangement.

In this work, we have investigated carbon aerosols produced in various residence times in the flame by TOT measurements and Raman spectroscopy to characterize their structural composition and optical properties in correlation with their OC and EC content.

Experimental

In this study, an analysis of carbonaceous nanoparticles produced in a premixed laminar ethylene-air flame was conducted. The flame was stabilized on a water-cooled sintered steel McKenna burner with a diameter of 6 cm, where the cold gases reached the burner at a velocity of 9.8 cm/s. The chosen fluxes led to a flame characterized by a (C/O) atomic ratio of 0.67, $\phi=2.01$. To collect the particles, a tubular dilution stainless-steel probe constituted by an orifice with diameter of 0.6 mm was employed, allowing for the extraction of carbonaceous particles from the flame centerline. The sampled flow was mixed immediately with a turbulent N₂ diluent flow, achieving a dilution ratio on the order of 1:350, and then directed to a filter holder containing a 47 mm pre-fired quartz filter. A representation of the experimental setup is depicted in Fig. 1a.

The premixed flame enabled the collection of combustion products at various distances from the burner surface, Z , corresponding to different residence times. Nanoparticles were collected from $Z=6$ mm to $Z=10$ mm, with each filter undergoing a total sampling duration of 5 hours. Subsequently, the particles collected on the quartz filter underwent offline characterization through TOT and Raman measurements.

For TOT analysis, a rectangular filter piece (1.5×1 cm) from the central portion of the filter was utilized with a Lab OC-EC Aerosol Analyzer from Sunset Laboratory Inc., following the NIOSH870 method. During the analysis, the sample undergoes two phases: first, the sample is exposed to He gas while the temperature is ramped up, causing OC to evolve from the filter and then, in an oxidized environment, to CO₂ a flame ionization detector (FID). After the first cooling phase, a mixture of helium and oxygen is introduced, and the temperature is ramped up in steps again. Some fraction of OC pyrolyzes rather than evaporate generating a pyrolytic carbon (PC). The PC is supposed to have similar optical properties of EC, so it has to be considered to avoid overestimating EC. The carbon generated during this oxidizing phase is converted to CH₄ for quantification and is defined as EC. After a second cooling phase, CH₄ is injected for FID signal calibration. Since OC and EC show different behavior in the visible region of light, a laser ($\lambda=670$ nm) monitors filter transmittance through the filter to separate PC from EC by defining a “split point”. Before the split point the measured signal is attributed to OC, after the split point is attributed to EC. The split point is numerically defined when laser transmittance equals the mean of the first 10 seconds of ambient temperature analysis.

Raman spectroscopy analysis was conducted using a Horiba XploRA Raman microscope system equipped with a 100 \times objective (NA 0.9, Olympus) and a frequency-doubled Nd: YAG laser ($\lambda = 532$ nm) as the laser source. To prevent structural changes in the sample due to thermal decomposition and ensure optimal resolution, laser beam power, exposure time, and other instrumental parameters were meticulously selected. Spectra were acquired with a laser beam power set at 10% of attenuation and an accumulation (exposure) time of five cycles, each lasting 30 seconds. Five randomly selected spots per sample were averaged to enhance statistical relevance, and all spectra were subsequently baseline-corrected and normalized to the maximum of the G peak at approximately 1600 cm^{-1} .

Results

Fig. 1a shows the outcomes of the filter sampling procedure. Next to the representation of the experimental setup, the images of five filters, coated with carbonaceous material, are presented. These filters are displayed sequentially, with increasing residence times, from bottom to top. A preliminary qualitative assessment reveals a progression in coloration from light brownish to darker brown, except for the visibly darker sample at $Z=9$ mm, which appears to diverge from this pattern.

In Fig. 1b the thermogram of the filter acquired at $Z=7$ mm is reported. In the first He phase the OC is determined. When the temperature increases again and with the oxidized ambient the PC is generated until the split point. After that, the carbon is defined as EC. The EC/TC and OC/TC ratio values gained from TOT analysis are reported in Table 1. The OC reported in table 1 has to be considered as $OC_{TOT} = OC + PC$. The data indicate a prevalence of organic carbon at lower residence times, particularly at $Z=6$ mm, where gas-phase molecular compounds dominate, and initial nucleation of molecules commences. With longer residence times, the organic

carbon content diminishes in favor of elemental carbon.

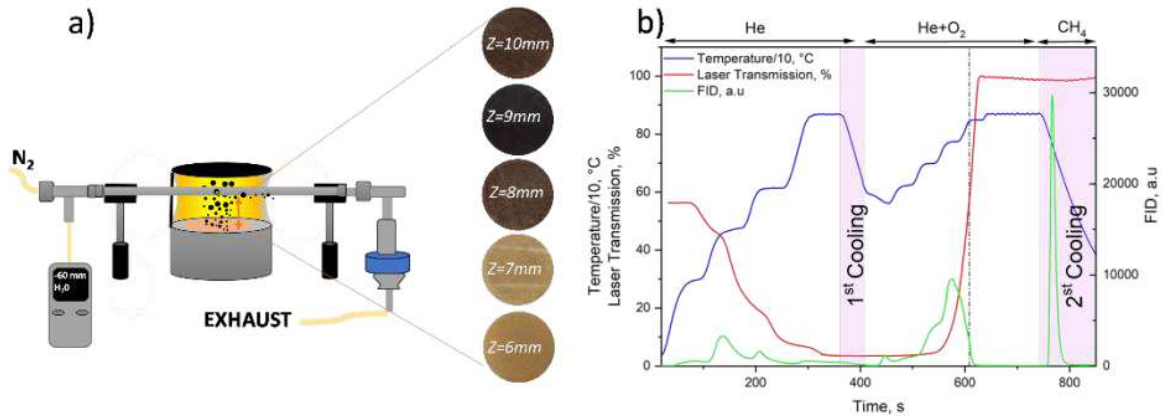


Figure 1 a) Experimental set-up on the left; filters acquired at different times on the right; b) Thermogram showing the ramp temperature program, blue line; measured laser transmission in red line; FID signal in green line. The vertical dashed line shows the split point which divides the EC from OC.

Table 1

Z, mm	EC/TC	OC/TC	m/I(G)	H/C
6	0.05±0.01	0.95±0.10	23.23 ±9.26	0.78±0.11
7	0.19±0.02	0.81±0.09	10.56±2.67	0.63±0.05
8	0.35±0.04	0.65±0.07	6.18±1.68	0.53±0.05
9	0.38±0.04	0.62±0.06	3.63±0.44	0.45±0.02
10	0.38±0.04	0.62±0.07	2.22±0.17	0.38±0.01

Fig. 2a displays the results of Raman spectroscopy. Each Raman spectrum exhibits the characteristic D and G bands typical of carbon compounds. It is noteworthy that the Raman spectra at lower residence times exhibit a split at the G-band, warranting further investigation. The fluorescence background contribution, reported in Table 1, is calculated from the Raman spectra and, consistent with the TOT findings, demonstrates a significant contribution at lower residence times, coinciding with the onset of nucleation, where organic carbon predominates. Indeed, as shown in Fig. 2b, an increasing trend in OC/TC as a function of photoluminescence is observed with a considerable difference between lower and higher residence time. In Table 1 also the Hydrogen to Carbon (H/C) ratio is reported. The H/C ratio, calculated from the m/I(G) and using Equation 1 [11], correlates with this trend, Fig. 2c. At lower residence time where is predominant the organic carbon fraction also the H furnishes its major contribution.

$$H[at. \%] = 21.7 + 16.6 * \log\left(\frac{m}{I(G)}\right) \quad (1)$$

As residence time increases, the particles approach a predominantly carbonaceous composition, with a gradual decrease in hydrogen and organic carbon contribution. The values derived from this investigation are in close agreement with the existing literature [12, 13].

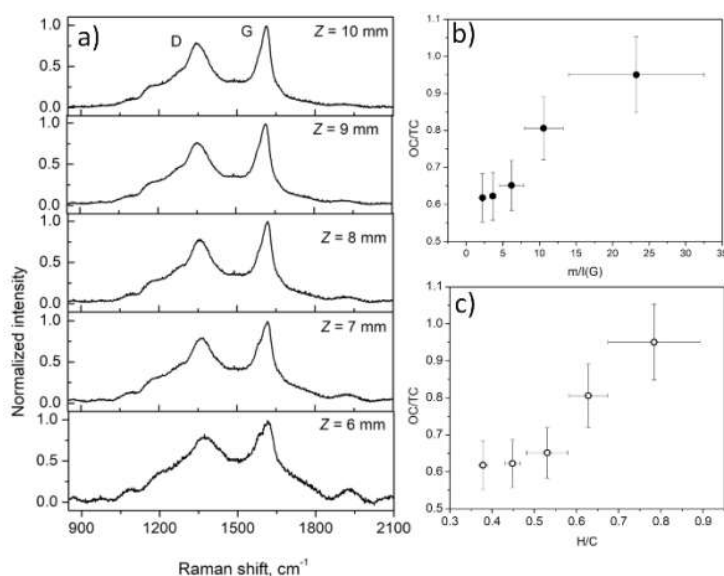


Figure 2 a) Raman spectra of all the 5 acquired filters; b) representation of OC/TC ratio as a function of m/I(G); c) representation of OC/TC ratio as a function of H/C.

Conclusions

The combined use of TOT analysis and Raman spectroscopy allows for describing the evolution of OC and EC fractions as a function of residence time within a lightly sooting laminar premixed ethylene/air flame. The results underscore the prevalence of organic carbon at the early stages of particle formation, transitioning to elemental carbon increasing at higher residence time. The joint of these two techniques reveals quite marked differences in chemical composition among the generated particles. Where the photoluminescence is higher, there is a great H contribution derived from mainly organic carbon. These conditions, rich in H, could be the ideal set in the nucleation step, through polymerization reaction by aromatic radical involvement. Conversely, at higher residence times, aligning with the formation of more coagulated, aggregated nanoparticles, the variation in organic carbon content, H percentage, and photoluminescence signals appear well correlated to each other. Nevertheless, the relative intensity of the two main Raman signals, the D and the G bands typically used to follow graphitization and/or the amorphization of carbonaceous materials, remains mostly unchanged in the examined conditions. The process of carbonization and dehydrogenation occurring during the early evolution of the nascent soot does not involve the planar growth of the aromatic constituents but probably mainly the formation of cross-links through the aromatic domains composing the particles. This, in turn, may be responsible for the change of optical, electronic, and other physical properties of the particles during their evolution in

flame often observed in the literature.

Acknowledgment This work was supported by PRIN – “Investigating atmospheric fate and Toxicological properties of Biofuels Emitted ultrafine particles with a SimulaTion chamber (IT-BEST)”

References

- [1] Abid, A.D., Heinz, N., Tolmachoff, E.D., Phares, D.J., Campbell, C.S., Wang, H.: “On evolution of particle size distribution functions of incipient soot in premixed ethylene-oxygen-argon flames”, *Combust Flame*. 154: 775-788 (2008).
- [2] Commodo, M., De Falco, G., Bruno, A., Borriello, C., Minutolo, P., D’Anna, A.: “Physicochemical evolution of nascent soot particles in a laminar premixed flame: From nucleation to early growth”, *Combust Flame*. 162: 3854–3863 (2015).
- [3] Gu, C., Lin, H., Camacho, J., Lin, B., Shao, C., Li, R. et. al. “Particle size distribution of nascent soot in lightly and heavily sooting premixed ethylene flames”, *Combust Flame*. 165: 177–187 (2016).
- [4] Commodo, M., De Falco, G., Minutolo, P., D’Anna, A., “Structure and size of soot nanoparticles in laminar premixed flames at different equivalence ratios”, *Fuel*. 216: 456–462 (2018).
- [5] Bond, T.C., Doherty, S.J., Fahey, D.W., Forster, P.M., Berntsen, T., Deangelo, B.J., et al., “Bounding the role of black carbon in the climate system: A scientific assessment”. *J. Geophys. Res.* 118: 5380–5552 (2013).
- [6] Murayama, H., Tomonoh, S., Alford, J.M., Karpuk, M.E., “Fullerene production in tons and more: From science to industry” *Fuller.Nanotub. Carbon Nanostructures* 12:1-9 (2004).
- [7] Memon, N.K., Tse, S.D., Al-Sharab, J.F., Yamaguchi, H., Goncalves, A.M.B., Kear, et al. “Flame synthesis of graphene films in open environments”. *Carbon*. 49: 5064-5070 (2011).
- [8] Liu, H., Ye, T., Mao, C., “Fluorescent carbon nanoparticles derived from candle soot” *Angew.Chem.Int.Ed.* 46:6473-6475 (2007).
- [9] Minutolo, P., Gambi, G., D’Alessio, A., “The optical band gap model in the interpretation of the UV-visible absorption spectra of rich premixed flames”. *Symposium (International) on Combustion*. 26: 951–957 (1996).
- [10] Bocchicchio, S., Commodo, M., Sgro, L.A., Chiari, M., D’Anna, A., Minutolo, P., “Thermo-optical-transmission OC/EC and Raman spectroscopy analyses of flame-generated carbonaceous nanoparticles” *Fuel*. 310: 122308 (2022).
- [11] Casiraghi, C., Piazza, F., Ferrari, A.C., Grambole, D., Robertson, J., “Bonding in hydrogenated diamond-like carbon by Raman spectroscopy”, *Diam Relat Mater*. 14:1098-1102 (2005).
- [12] Faccinetto, A., Irimiea, C., Minutolo, P., Commodo, M., D’Anna, A., Nuns, N., et al. “Evidence on the formation of dimers of polycyclic aromatic hydrocarbons in a laminar diffusion flame” *Commun Chem*. 3, (2020).
- [13] Buijnsters, J.G., Gago, R., Jiménez, I., Camero, M., Agulló-Rueda, F., Gómez-Aleixandre, C., “Hydrogen quantification in hydrogenated amorphous carbon films by infrared, Raman, and x-ray absorption near edge spectroscopies” *J Appl Phys*. 105, 093510 (2009).